

²³Na, ²⁹Si, and ¹³C MAS NMR Investigation of Glass-Forming Reactions between Na₂CO₃ and SiO₂

Aled R. Jones,^{†,§} Rudolf Winter,^{*,†} G. Neville Greaves,[†] and Ian H. Smith[‡]

Materials Physics, University of Wales Aberystwyth, Penglais, Aberystwyth SY233BZ, Wales, United Kingdom, and Pilkington plc, Pilkington Technical Centre, Hall Lane, Lathom, Lancashire L405UF, England, United Kingdom

Received: July 18, 2005; In Final Form: October 15, 2005

The glass-forming reactions between sodium carbonate (Na₂CO₃) and silica (SiO₂) have been investigated by ²³Na, ²⁹Si, and ¹³C magic-angle spinning (MAS) NMR spectroscopy. The multinuclear MAS NMR approach identifies and quantifies reaction products and intermediates, both glassy and crystalline. A series of powdered batches of initial composition Na₂CO₃·xSiO₂ (x = 1, 2) corresponding to a sodium metasilicate (Na₂SiO₃) and sodium disilicate (Na₂Si₂O₅) stoichiometry were investigated after periods of isothermal and nonisothermal heat treatments at different temperatures. Analysis of the ²³Na quadrupolar coupling parameters has identified the early reaction product in all cases as crystalline Na₂SiO₃. In the nonisothermal experiment, this reaction is preceded by an early silica-rich melt phase formed around 850 °C. The early reactions are controlled by solid-state Na⁺ diffusion across the reaction zone in the grain interface layer. Crystalline Na₂SiO₃ precipitates in the interface layer, increasing its thickness between the Na₂CO₃ and the SiO₂ grains and slowing down the rate of Na⁺ migration. This creates a secondary phase, which is temperature dependent. At low temperatures, where Na⁺ migration is impaired, the production of Na₂SiO₃ ceases and silica-rich phases are precipitated. In the case of the sodium disilicate batch, where excess SiO₂ is present, a secondary reaction of Na₂SiO₃ with SiO₂ forming a glassy phase is observed. A transient carbon-bearing phase has been identified by ¹³C NMR as a NaCO₃[−] complex loosely bound to bridging oxygens in the silicate network at the SiO₂ grain surface.

1. Introduction

Chemical reactions involving powdered batches are subject to a number of physical constraints that cause a deviation from equilibrium chemistry. Such reactions can be purely solid state, in which case diffusion across the boundary layer or interface between the grains plays a major role as well as the malleability of the reactant grains as it determines the active surface area, i.e., the actual contact cross section between adjacent reactant grains. Alternatively, a reactant or a product phase produced by a solid-state reaction may melt, leading to a solid–liquid interface reaction controlled by diffusion as well as surface tension and wetting of the remaining grains by the liquid formed. As a consequence, these physical constraints will determine whether the reaction is kinetically or thermodynamically controlled. This investigation focuses on the role grain surfaces and interfaces play in batch melting reactions of glass-forming silicate batches. The term *interface layer* will be used to describe the reaction zone near the surface of the quartz grains in which Na⁺ diffusion may take place.

Commercially, a full understanding of the melting characteristics of a soda-lime silicate glass batch has considerable importance. Fundamental to this understanding is the identification and quantification of the various reactions that occur on heating the batch. A significant challenge is the development of a technique that can identify and quantify these reactions,

intermediates, and reaction products. Experimental studies have investigated glass-forming reactions utilizing mainly thermogravimetric analysis (TGA) and differential thermal analysis (DTA).^{1–7} TGA experiments monitor the mass loss of the reacting batch, i.e., the amount of CO₂ evolved. As the CO₂ is released fairly early on in the process, TGA is rather limited in establishing full reaction pathways. Other work has investigated the dissolution of vitreous silica rods in melts of pure Na₂CO₃, Na₂CO₃ + CaCO₃, and Na₂CO₃ already reacted with small proportions of silica.⁸ A limited number of studies have attempted to quantify the intermediate phases by X-ray diffraction (XRD) methods^{4–6,9} including in situ diffraction¹⁰ and electron microscope microanalysis (EMMA)¹¹ as well as our own ex situ¹² and in situ¹³ static NMR work.

Solid-state magic-angle spinning nuclear magnetic resonance spectroscopy (MAS NMR) has been a widely used technique for the investigation of homogeneous glassy systems including silicates for some time.^{14–17} A fundamental aspect of ²⁹Si MAS NMR in silicate systems is the identification of various silicate tetrahedra with varying numbers, *n*, of bridging oxygens, commonly described as Q^{*n*} species. ²³Na MAS NMR spectra are less easily interpreted as to the specific chemical environments surrounding the ²³Na nuclei as the lines are broadened not only by the distribution of bond angles in an amorphous system but also due to the inability of MAS NMR to eliminate fully the effects of second-order quadrupolar interactions. However, in a crystalline structure, the range of bond angles will be restricted, and the resonance will be considerably narrower than the corresponding amorphous structure. Line shape analysis of the resonance is therefore possible, and the quadrupolar coupling parameters C_Q and η_Q (quadrupolar

* Author to whom correspondence should be addressed. Phone: +44-1970-62-1797. Fax: +44-1970-62-2826. E-mail: ruw@aber.ac.uk.

[†] University of Wales Aberystwyth.

[‡] Pilkington plc.

[§] Present address: Pilkington plc.

coupling constant and asymmetry parameter) can be determined. MAS NMR is well suited to investigate the reaction products of a sodium silicate glass batch because it gives not only quantitative information on the reaction product formed but also structural information on the local environment of the probe nuclei as the progressive change from batch to glass takes place. Therefore, a multinuclear MAS NMR approach with ^{29}Si , ^{23}Na , and ^{13}C MAS NMR has been used in this study as a quantitative technique to investigate the intermediate crystalline and amorphous phases formed during the reaction of Na_2CO_3 and SiO_2 to produce a glass.

^{13}C MAS NMR is particularly useful for the study of transient phases during the sintering and melting process because carbon is released as CO_2 before the reaction completes and, hence, any spectral lines appearing other than for the reactant itself must originate from an intermediate product. There are, however, only a few ^{13}C studies because of the difficulties arising from the very slow spin–lattice relaxation of the nucleus. The problem can be overcome partially by signal enhancement through polarization transfer from protons, a technique that has been used in sol–gel based silicates,¹⁸ or by isotopic enrichment if the sample does not contain many protons, the route chosen here. In previous studies, the application of ^{13}C NMR incorporated in glass has been focused on volatiles in silicate melts.^{19–22} Such experiments have studied the solubility and speciation of carbon dioxide in natural magmatic systems, with the aim of understanding their behavior in melts and the role they play in magmas. From thermodynamic considerations²³ it is clear that geological pressures are needed to dissolve any CO_2 , molecular or otherwise, in a silicate melt. The volatile solubility experiments involve exposing the silicate melt to high pressure and high temperature in the presence of a CO_2 source, e.g., alkali carbonates, which ensures, in conjunction with the pressure applied, that the system is saturated with molecular CO_2 . The melts are subsequently quenched and analyzed for any dissolved carbon-containing species. These solubility and speciation studies typically use samples prepared from the corresponding oxides and carbonates and subjected to pressures varying from 10 to 25 kbar on heating with an excess of liquid CO_2 . These studies are used as shift references to interpret the spectra of the carbon-containing intermediate in a glass-forming batch presented here for the first time.

2. Experimental Section

Throughout the text, crystalline phases will be referred to by their sum formula (e.g., Na_2SiO_3), while batches and glasses will be referred to by their components separated by hyphens and dots, respectively (e.g., $\text{Na}_2\text{CO}_3\text{--SiO}_2$ batch, glassy $\text{Na}_2\text{O}\cdot\text{SiO}_2$).

2.1. Nonisothermal Sample Preparation. $\text{Na}_2^{13}\text{CO}_3\text{--SiO}_2$ (metasilicate batch) mixtures were prepared from high purity quartz and 99% ^{13}C -enriched Na_2CO_3 (Euriso-Top, France). The quartz particle size was chosen in the range of 63 to 90 μm diameter, obtained by sieving. This provided sufficient quartz surface area to encourage solid-state reaction. To all samples, 0.15 wt % of Fe_2O_3 was added to reduce the spin–lattice relaxation time, T_1 , of the ^{29}Si in the reaction phase. Samples of 200 mg of batch were heated in a platinum crucible at a rate of 10 K min^{-1} and air-quenched from 700, 850, 950, 1090, and 1300 $^\circ\text{C}$. The small amount of sample used ensured a uniform heating of the batch and a rapid quench rate so that no devitrification of any melt phases would occur.

2.2. Isothermal Sample Preparation. $\text{Na}_2\text{CO}_3\text{--SiO}_2$ (metasilicate batch) and $\text{Na}_2\text{CO}_3\text{--}2\text{SiO}_2$ (disilicate batch) mixtures

were prepared with 63 to 90 μm high purity quartz and standard reagent grade Na_2CO_3 . Again, 0.15 wt % of Fe_2O_3 was added. Three series of samples were prepared from the raw glass batches: $\text{Na}_2\text{CO}_3\text{--SiO}_2$ heated at 700 $^\circ\text{C}$ and $\text{Na}_2\text{CO}_3\text{--}2\text{SiO}_2$ heated at 775 and 850 $^\circ\text{C}$. These will be referred to as M700, D775, and D850, respectively. All 200 mg samples were quenched after various periods of heat treatment.

2.3. MAS NMR. ^{29}Si , ^{23}Na , and ^{13}C spectra were collected on a Bruker Avance DSX400 NMR spectrometer with a 9.4T cryomagnet at resonance frequencies of 79.5, 105.8, and 100.6 MHz, respectively. Rotor spinning rates of 5, 15, and 10 kHz were used for ^{29}Si , ^{23}Na , and ^{13}C , respectively.

^{29}Si spectra were acquired with a 30 $^\circ$ flip angle and recycle delays varying with the sample studied. Since the Fe_2O_3 is only incorporated into the reacted or melted phases of the samples, the Fe ions have virtually no effect on the spin–lattice relaxation of the ^{29}Si nuclei in SiO_2 . Therefore, the relaxation time, T_1 , in product phases is reduced due to spin diffusion to the paramagnetic centers followed by nuclear–electronic dipolar relaxation. Hence, by employing a suitably short recycle delay the NMR detection is selective to the newly formed phases since the ^{29}Si nuclei in raw SiO_2 do not have sufficient time to relax between scans. To observe the SiO_2 resonance, a delay of 400 s has been used in some experiments, but even then the SiO_2 intensity is attenuated relative to the other resonance lines. This means that quantitative measurements of SiO_2 in the sample are not possible from the ^{29}Si spectra. Spectra were referenced to tetramethylsilane (TMS) at 0 ppm.

^{23}Na spectra acquired with a $\pi/12$ pulse ensure a quantitative excitation of the central transition of all the ^{23}Na sites. ^{23}Na nuclei have very efficient relaxation mechanisms and quantitative spectra could therefore be obtained. Spectra were referenced to 1 mol L^{-1} aqueous NaCl at 0 ppm.

^{13}C spectra suffer from similarly long relaxation times as ^{29}Si spectra. Full relaxation of the spins between scans was not practical. ^{13}C spectra were typically acquired with a $\pi/6$ pulse, recycle delay of 800 s, and 6 signals averaged. Chemical shifts are referenced to TMS at 0 ppm.

3. Results

3.1. Nonisothermal Batches. The ^{29}Si MAS NMR spectra for the $\text{Na}_2^{13}\text{CO}_3\text{--SiO}_2$ batch samples subjected to progressive heating and subsequently quenched from 700, 850, 950, 1090, and 1300 $^\circ\text{C}$ are illustrated in Figure 1a. The spectrum of the unheated batch (i.e., the spectrum of SiO_2) is also shown for comparison and is characterized by one narrow line at -107 ppm. The spectra clearly illustrate that progressive heat treatment promotes the formation of a second narrow line at -77 ppm. This resonance possesses a chemical shift that is expected for crystalline Na_2SiO_3 ,²⁴ therefore the line is assigned to this compound, which can be described as a crystalline Q^2 . The growth of this crystalline Q^2 line is accompanied by a reduction in the intensity of the SiO_2 or crystalline Q^4 line at -107 ppm.

The spectrum of the sample quenched from 850 $^\circ\text{C}$ in Figure 1a was acquired with a delay of 400 s between consecutive data acquisitions, therefore allowing a partial relaxation of the ^{29}Si nuclei in SiO_2 . The signal-to-noise is poor due to only 170 spectra being acquired and averaged owing to the long delay. A spectrum of the 850 $^\circ\text{C}$ sample with a 25 s delay and 4500 averaged spectra was also acquired and is illustrated in Figure 1b. The signal-to-noise is improved and all the reaction products can be identified. However, the SiO_2 peak has lost intensity due to the long ^{29}Si T_1 relaxation time in pure unreacted SiO_2 . A broad resonance peak centered at about -90 ppm is attributed

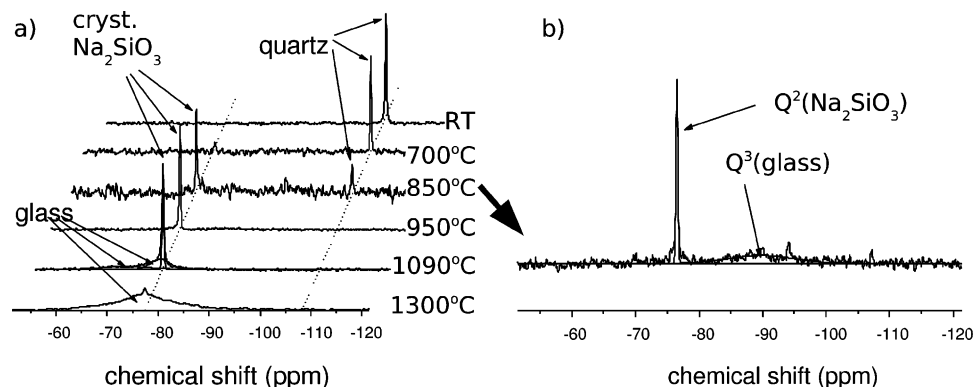


Figure 1. (a) ^{29}Si MAS NMR spectra of the nonisothermal batch heated at 10 K min^{-1} to the specified temperatures. (b) A spectrum of the sample quenched at $850\text{ }^{\circ}\text{C}$, acquired with a shorter recycle delay than in part a, together with Gaussian fit components.

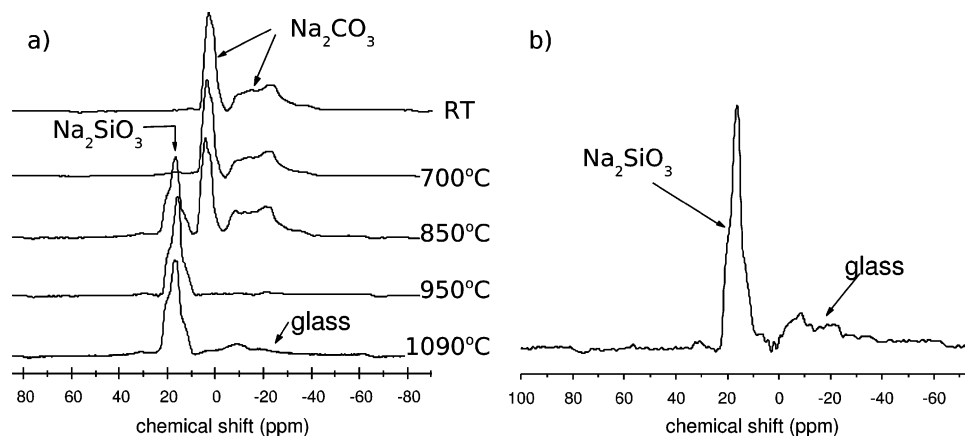


Figure 2. (a) ^{23}Na MAS NMR spectra of the nonisothermal batch heated at 10 K min^{-1} to the specified temperatures. (b) The spectrum of the sample quenched at $850\text{ }^{\circ}\text{C}$ after subtraction of the spectrum of the raw material, Na_2CO_3 .

to glassy Q^3 . In Figure 1a, the spectrum of the sample heated to $950\text{ }^{\circ}\text{C}$ was acquired with a 6 s delay since the T_1 time of the ^{29}Si nuclei in the Na_2SiO_3 reaction product is sufficiently short.

Thermal calcination of Na_2CO_3 is not expected in a glass-forming batch and will only take place with reaction with SiO_2 . Therefore, any change in the ^{23}Na line shape of the heat-treated $\text{Na}_2^{13}\text{CO}_3\text{-SiO}_2$ mixture must be due to a reaction product. ^{23}Na MAS NMR spectra of the $\text{Na}_2^{13}\text{CO}_3\text{-SiO}_2$ mixture heated at 10 K min^{-1} to 700, 850, 950, and $1090\text{ }^{\circ}\text{C}$ are illustrated in Figure 2a. The ^{23}Na spectrum of the unheated sample (i.e., Na_2CO_3 spectrum) is characterized by two peaks in the range 10 to -55 ppm . These are due to two crystallographic Na^+ sites in Na_2CO_3 .

Figure 2a shows the emergence of a peak at about 19 ppm and the demise of the Na_2CO_3 contribution as heat treatment progresses. Simulations of the peak near 19 ppm in all spectra were made with the program Dmfit.²⁵ This gives the quadrupolar coupling constant, $C_Q = (1.4 \pm 0.1)\text{ MHz}$, asymmetry parameter, $\eta_Q = 0.7 \pm 0.1$, and isotropic chemical shift, $\delta_{\text{iso}} = (20.0 \pm 0.5)\text{ ppm}$. This compares well with published values for crystalline Na_2SiO_3 prepared by devitrification.^{26,27} The spectrum of the sample heated to $950\text{ }^{\circ}\text{C}$ is characterized by only one peak, which is due to Na_2SiO_3 ; therefore, Na_2CO_3 is no longer present. However, a broad line re-emerges in the range 10 to -40 ppm in the spectrum of the sample heated to $1090\text{ }^{\circ}\text{C}$. The smoothed and slightly broadened line shape signifies a glassy component. This glassy phase is also evident in the corresponding ^{29}Si spectrum (cf. Figure 1a). A closer inspection of the ^{23}Na spectrum of the sample heated to $850\text{ }^{\circ}\text{C}$ reveals a slight change in the line shape between -5 and -15 ppm

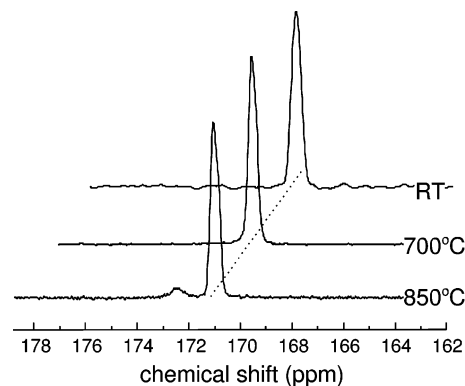


Figure 3. ^{13}C MAS NMR spectra of the (^{13}C -enriched) nonisothermal batch heated at 10 K min^{-1} to 700 and $850\text{ }^{\circ}\text{C}$. The spectrum of the raw batch (room temperature, RT) is shown for comparison. At higher temperatures, no ^{13}C signal is observable.

compared to spectra of the unheated sample and the sample heated to $700\text{ }^{\circ}\text{C}$. This is clearly visible when the Na_2CO_3 component of the spectrum is subtracted (using the narrow Na_2CO_3 resonance line to scale the contribution). The difference spectrum between the Na_2CO_3 spectrum and that of the sample heated to $850\text{ }^{\circ}\text{C}$ is illustrated in Figure 2b. A broad component is present between about 0 and -40 ppm , similar to that seen in the spectrum of the sample heated to $1090\text{ }^{\circ}\text{C}$. Therefore, a glass phase is formed in the sample heated to $850\text{ }^{\circ}\text{C}$, which subsequently disappears by $950\text{ }^{\circ}\text{C}$ followed by the formation of a new glass phase in the sample heated to $1090\text{ }^{\circ}\text{C}$.

^{13}C MAS NMR spectra are illustrated in Figure 3 for the unheated $\text{Na}_2^{13}\text{CO}_3\text{-SiO}_2$ mixture and samples heated to 700 and $850\text{ }^{\circ}\text{C}$, respectively. The resonance of $\text{Na}_2^{13}\text{CO}_3$ has a peak

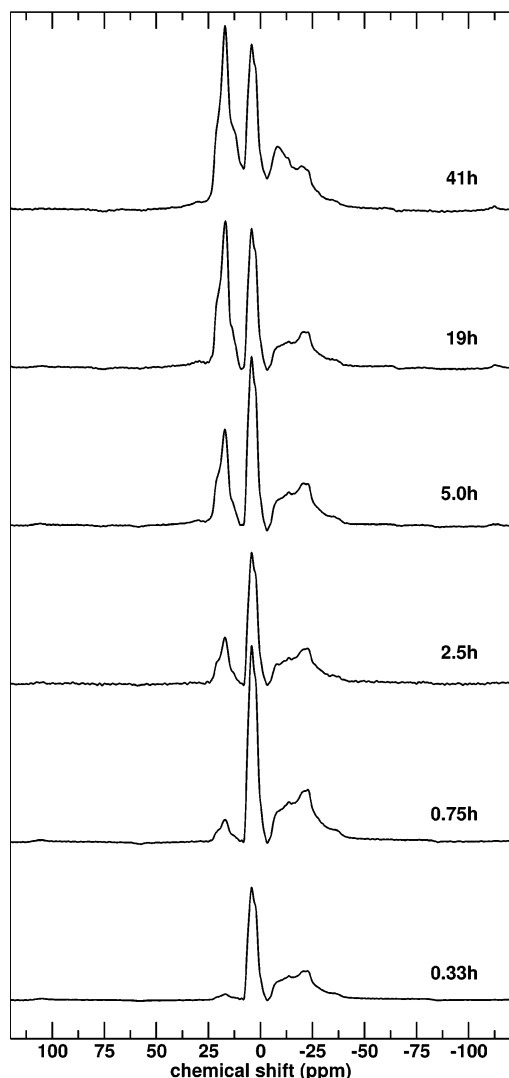


Figure 4. ^{23}Na MAS NMR spectra of isothermal metasilicate batch reacted at 700 °C for the periods indicated.

maximum at 170.7 ppm and a full width at half magnitude (fwhm) of 0.4 ppm. The sample heated to 700 °C shows no change in line shape or position. However, the spectrum of the sample heated to 850 °C shows an additional peak at 172.1 ppm with an fwhm of 0.7 ppm. The relaxation of both lines is very slow; complete relaxation of the raw material's contribution was not observed after 9 h. Therefore, a quantitative analysis of the relative strength of the two peaks is not possible. However, the T_1 value of the peak at 172.1 ppm was measured to be 200 s. This indicates that the ^{13}C nuclei are in closer proximity to the paramagnetic ions that facilitate the ^{13}C nuclei to dissipate their energy and hence reduce the T_1 time. No ^{13}C signal is detectable in samples heated beyond 850 °C.

3.2. Isothermal Metasilicate Batch. Illustrated in Figure 4 are ^{23}Na MAS NMR spectra of the $\text{Na}_2\text{CO}_3\text{-SiO}_2$ series of samples isothermally heated at 700 °C (M700). The first sample was heated for 20 min, and the onset of crystalline Na_2SiO_3 formation is identified by the resonance line centered near 20 ppm. The growth of the Na_2SiO_3 peak is observed with increasing heat treatment at the expense of the Na_2CO_3 contribution. The value of the asymmetry parameter, $\eta_Q = 0.7 \pm 0.1$, and that of the quadrupolar coupling constant, $C_Q = (1.4 \pm 0.1)$ MHz, are consistent with crystalline Na_2SiO_3 in each spectrum. However, there is a significant difference in the ^{23}Na MAS NMR line shape of the sample heated for 41 h, with

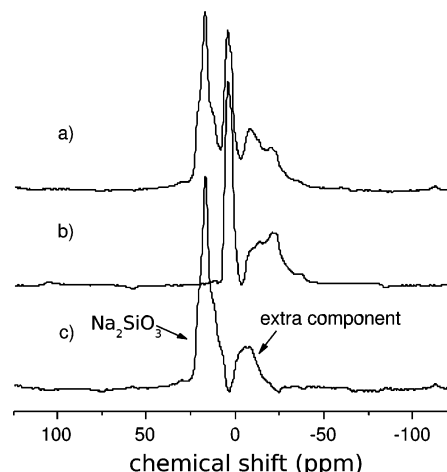


Figure 5. ^{23}Na MAS NMR spectra of (a) the isothermal metasilicate batch reacted at 700 °C for 41 h and (b) the raw material, Na_2CO_3 . (c) Difference spectrum, i.e., the batch spectrum after subtraction of the contribution from unreacted raw material.

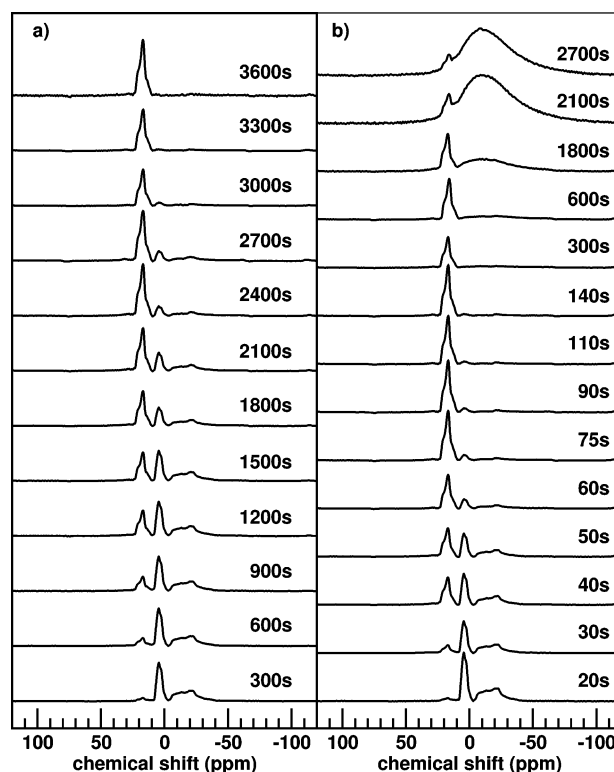


Figure 6. ^{23}Na MAS NMR spectra of the isothermal disilicate batch reacted for the periods indicated at (a) 775 and (b) 850 °C.

a broadening at the base of the resonance lines. Subtracting the Na_2CO_3 contribution from this line shape (using the narrow Na_2CO_3 resonance line to scale the contribution) as illustrated in Figure 5 can separate this additional component. The difference spectrum clearly shows the resonance line of Na_2SiO_3 , together with an additional resonance line centered near -10 ppm, which is distinctly narrower than the glassy residual phase found in the nonisothermal experiment (cf. Figure 1b). This indicates that changes of the local environment surrounding some ^{23}Na atoms occur only after 41 h of heating.

3.3. Isothermal Disilicate Batches. Illustrated in Figure 6a are ^{23}Na MAS NMR spectra of the $\text{Na}_2\text{CO}_3\text{-2SiO}_2$ mixture heated at 775 °C (D775). Eleven samples were prepared in total by heating the mixture for periods ranging between 5 and 60

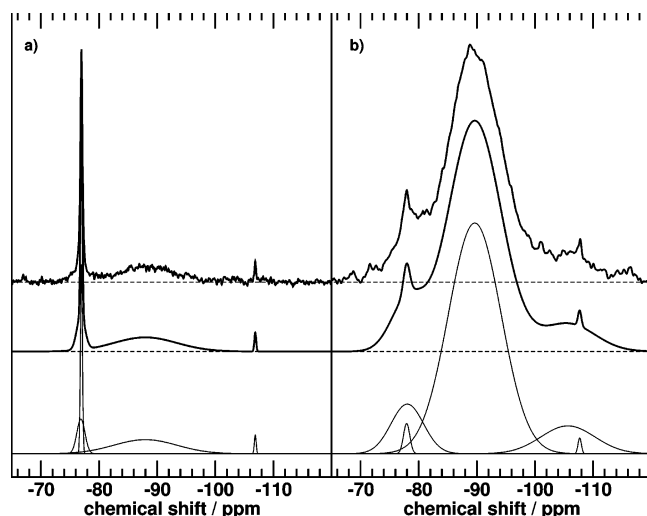


Figure 7. ^{29}Si MAS NMR spectrum of the isothermal disilicate batch reacted at 850 °C for (a) 5 and (b) 35 min with model fits comprising crystalline SiO_2 and Na_2SiO_3 and amorphous $\text{Na}_2\text{O}\cdot 2\text{SiO}_2$ components.

min. Crystalline Na_2SiO_3 is produced at a substantially increased rate; Na_2SiO_3 is already detectable after 5 min of heating. Na_2CO_3 is fully reacted after 60 min leaving only crystalline Na_2SiO_3 and the remaining SiO_2 .

The spectra of the $\text{Na}_2\text{CO}_3\cdot 2\text{SiO}_2$ mixtures heated at 850 °C (D850), i.e., near the melting point of Na_2CO_3 , are shown in Figure 6b. The time scale of the reaction is much shorter than that in the previous experiments. After only 20 s, 5 mol % of crystalline Na_2SiO_3 has formed. The reaction between SiO_2 and Na_2CO_3 continues until all the Na_2CO_3 has reacted and only Na_2SiO_3 and the excess SiO_2 are left. The complete reaction of Na_2CO_3 takes only about 140 s. The spectral line shapes of the samples heated to 140 s are identical with those of the D775 series. They are characterized only by the emerging line due to crystalline Na_2SiO_3 and the diminishing Na_2CO_3 contribution. The D850 samples were further heated after the Na_2CO_3 had completely reacted. The spectra of these samples correspond to those heated for between 140 s and 45 min. After 300 s of heating a broad line appears close to the position of the original Na_2CO_3 resonance. The intensity increases with heating time at the expense of the crystalline Na_2SiO_3 resonance line. The new line centered near -15 ppm is very broad and, therefore, due to an amorphous phase.

^{29}Si spectra of the D850 samples heated for 5 and 35 min are illustrated in Figure 7, fitted with Gaussian components. The sharp resonance lines positioned at -77 and -107 ppm are due to crystalline Na_2SiO_3 and SiO_2 , respectively. Additionally, in Figure 7a, there is a broad line between the crystalline peaks due to the formation of a melt. This peak can be fitted with one Gaussian component positioned near -90 ppm, which is at a chemical shift position expected for Q^3 species. The intensity of the broad component is considerably greater in the spectrum in Figure 7b, indicating an increased amount of glassy phase. It is also apparent that three Gaussian components are needed to fit the glassy component positioned at -78, -90, and -106 ppm. These relate to chemical shifts expected of Q^2 , Q^3 , and Q^4 species, respectively. These glass phases match those observed in the ^{23}Na MAS NMR spectra.

4. Discussion

4.1. Nonisothermal Batches. ^{29}Si experiments with a 400 s delay show no contribution from SiO_2 in the sample heated to 950 °C. This proves that all the SiO_2 has reacted and only

crystalline Na_2SiO_3 is present by 950 °C. The formation of an increasing amount of glassy phase is observed as the sample is heated past the melting temperature of Na_2SiO_3 . The sample heated to 1300 °C illustrates the broadening of the resonance line due to the greater range of bond angle distribution in the glassy Na_2SiO_3 structure compared to the crystalline equivalent. Some crystalline Na_2SiO_3 remains at 1300 °C and is clearly seen as a narrow peak on top of the broad resonance peak in the bottom trace of Figure 1a.

A fully quantitative analysis of the ^{29}Si spectra containing unreacted SiO_2 is not possible due to the ^{29}Si in the SiO_2 not fully relaxing. This manifests itself by attenuating the SiO_2 peak intensity in the spectra. Full relaxation of the ^{29}Si nuclei in all phases present was only observed for the sample heated to 1300 °C, making a quantitative analysis possible. Hence, the amounts of various Q^n species were determined together with the amount of crystalline Na_2SiO_3 . The ^{23}Na spectra were used to determine the quantity of the various phases present for the remaining spectra, where full ^{29}Si relaxation was not observed.

Illustrated in Figure 8a are the contributions (mol %) of the different phases in the sample as a function of time determined from the ^{29}Si and ^{23}Na spectra. Details of the calculation of the fractions at 850 °C are given in the Appendix. The occurrence of a Q^1 species in the 1090 °C sample, which unbalances the average fraction of nonbridging oxygens, \bar{n} , suggests that a small amount of unreacted quartz has not been detected. The upper limit of this contribution, whose exact line width is difficult to determine due to the low signal-to-noise, is 14%, corresponding to 7% unreacted quartz, as indicated in Figure 8a. The schematic in Figure 8b illustrates the possible reaction path and intermediate compounds formed on heating of the $\text{Na}_2\text{CO}_3\cdot\text{SiO}_2$ mixture.

At 700 °C a solid-state reaction between SiO_2 and $\text{Na}_2^{13}\text{CO}_3$ begins to form crystalline Na_2SiO_3 . This is evident in the ^{29}Si spectrum with the line appearing at -77 ppm and from the ^{23}Na spectrum with the line appearing at about 19 ppm attributed to Na_2SiO_3 . The formation of Na_2SiO_3 increases as a function of heating at the expense of the SiO_2 and Na_2CO_3 . This is observed in both ^{29}Si and ^{23}Na spectra with a decrease in the relative intensities of the SiO_2 and Na_2CO_3 lines, respectively. The first occurrence of a glass phase is observed at 850 °C, therefore indicating the formation of a silicate melt. This relates to the broad peak in the ^{29}Si spectra centered at -90 ppm (Q^3) corresponding to the chemical composition of $\text{Na}_2\text{O}\cdot 2\text{SiO}_2$. The formation of this glass phase could be due to the melting of an equivalent crystalline phase, further reaction of the Na_2SiO_3 with SiO_2 , or a reaction of a liquid film of Na_2CO_3 wetting the quartz grains. Crystalline $\text{Na}_2\text{Si}_2\text{O}_5$ melts at 874 °C, therefore it is thermodynamically possible for this compound to precipitate following the reaction of SiO_2 and Na_2CO_3 between 700 and 850 °C. This would then melt when approaching its actual melting point, producing the glass phase observed after quenching. However, as no solid silica-rich intermediate product is directly observed, it is more likely that a reaction at the interface of the crystalline Na_2SiO_3 and SiO_2 grains leads to the formation of glassy $\text{Na}_2\text{O}\cdot 2\text{SiO}_2$. This glass phase then disappears at higher temperatures and is replaced by other glass phases. By 950 °C, both SiO_2 and Na_2CO_3 have fully reacted since the SiO_2 signal at -107 ppm has disappeared from the ^{29}Si spectra and no Na_2CO_3 contribution is present in the ^{23}Na spectra. The sample is composed only of crystalline Na_2SiO_3 at 950 °C. The silicate glass ($\text{Na}_2\text{O}\cdot 2\text{SiO}_2$) observed in the 850 °C sample is no longer present. This indicates a reaction of $\text{Na}_2\text{O}\cdot 2\text{SiO}_2$ with Na_2CO_3 to form crystalline Na_2SiO_3 , which is the thermodynamically stable product at this temperature. A significant change in the

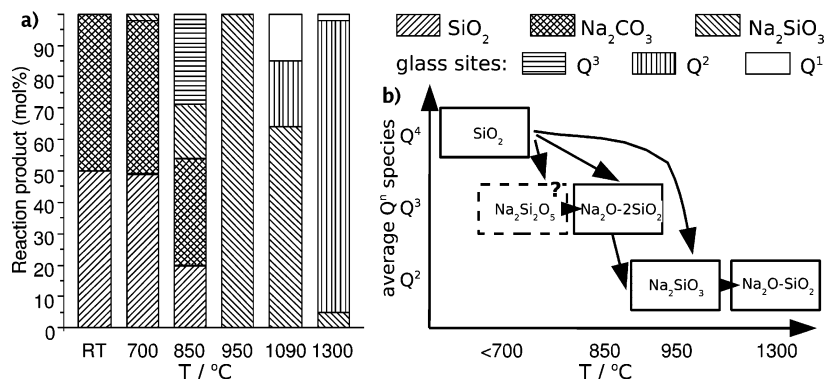


Figure 8. (a) Abundance of crystalline and glassy phases in the nonisothermal batch as a function of temperature reached based on the Q^n speciation derived from ^{29}Si experiments. (b) The reaction path reconstructed from the evolution of ^{29}Si and ^{23}Na spectra. See text for details.

^{29}Si spectra appears above the melting point of Na_2SiO_3 , at 1090 °C. A broad resonance peak due to a glass phase is observed corresponding to the melting of the crystalline Na_2SiO_3 structure. The broadness of the peak reflects the disordered environment of the ^{29}Si atoms in the newly formed melt/glass. By 1300 °C, virtually all of the crystalline Na_2SiO_3 has melted to form a homogeneous Q^2 glass.

The brief appearance of a second peak in the ^{13}C spectrum at 850 °C and its much shorter relaxation time in comparison to that of the reactant points to the fact that this contribution is due to a transient phase that exists only for a short time immediately before the ^{13}C is released as CO_2 . The only source of paramagnetic ions is 0.15 wt % of Fe_2O_3 introduced into the sample to reduce the T_1 value of the reaction products. These Fe_2O_3 particles would therefore be in contact with the SiO_2 and Na_2CO_3 grain surfaces. Hence, the interaction of the ^{13}C nuclei with paramagnetic centers suggests that the resonance at 172.1 ppm is due to ^{13}C nuclei in the interface layer. The change in chemical shift associated with this resonance line indicates that the ^{13}C chemical environment in this phase is somewhat different from that in the bulk Na_2CO_3 due to interactions of the carbonate with the silicate network. Molecular CO_2 can be ruled out as a possible origin of the peak since its line would occur at 125 ppm.¹⁹ High-pressure CO_2 saturation studies²⁰ also describe a resonance peak in the range 171 to 175 ppm. The authors suggest to relate this peak to a Na-carbonate ionic complex, i.e., a structural unit where the Na^+ is more closely connected with one of the carbonate ion's oxygen atoms, resulting in a reduced coordination number of the Na^+ ion. The formation of such complexes has also been concluded from Raman spectra of albitic and anorthic glasses.²⁸ Calculated ^{13}C NMR shielding values for various carbonate complexes in aluminosilicates²⁹ predict resonance peaks positioned between 155 and 175 ppm. At the lower end of the scale, peaks are assigned to CO_2 molecules attached to a bridging oxygen in the silicate network, while medium-range shifts correspond to carbonate ions forming part of the network themselves,^{19,30} i.e., where the carbonate oxygens are bridging oxygens connected to silicon neighbors. Values above the position of Na_2CO_3 itself are again ascribed to $(\text{NaCO}_3)^-$ complexes with reduced sodium coordination number. Therefore, the line observed here at 172.1 ppm is due to NaCO_3^- complexes incorporated in the interface layer which bond loosely to a bridging oxygen of the silicate network at the SiO_2 surface. CO_2 solubility is negligible unless under geological pressures.²³ In this study, no external pressure is applied. However, the ready supply of excess CO_2 from the decomposing Na_2CO_3 constitutes a driving force for CO_2 to dissolve temporarily in the silicate as $(\text{NaCO}_3)^-$ complexes by biasing the thermodynamic equilibrium. This dissolved CO_2 is

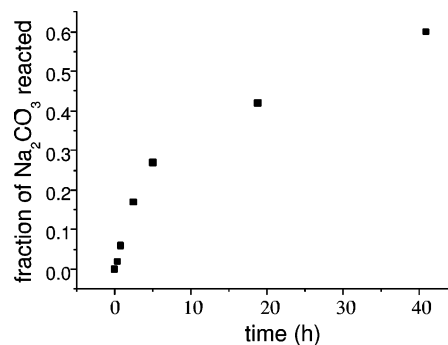


Figure 9. Fraction of raw material, Na_2CO_3 , reacted vs time for the isothermal metasilicate batch at 700 °C (M700).

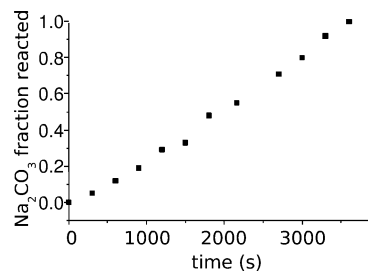


Figure 10. Fraction of raw material, Na_2CO_3 , reacted vs time for the isothermal disilicate batch at 775 °C (D775). Note the much shorter time scale than in Figure 9.

immediately released as soon as the CO_2 supply is exhausted and the thermodynamic equilibrium reinstated.

4.2. Isothermal Batches. The progress of the reaction of the isothermal batches is monitored by analyzing the quantitative ^{23}Na spectra. The fraction of Na_2CO_3 reacted as a function of time in metasilicate batch at 700 °C (M700) is shown in Figure 9. It is apparent that the rate of reaction is deceleratory and only about 60% of the Na_2CO_3 has reacted after 41 h.

The fraction of Na_2CO_3 reacted as a function of time in disilicate batch at 775 °C (D775) is illustrated in Figure 10. The reaction proceeds in approximately linear fashion until all Na_2CO_3 is consumed after about 1 h. The product is metasilicate, with excess quartz remaining after the end of the reaction.

In disilicate batch at 850 °C (D850), the reaction proceeds in a second step. Metasilicate is merely an intermediate product in this case; it reacts with the excess quartz by forming a glass. The buildup and decay of crystalline Na_2SiO_3 as a function of time is illustrated in Figure 11. The lower and upper time axes relate to the formation and decay of crystalline Na_2SiO_3 , respectively.

The formation of crystalline Na_2SiO_3 from the reaction of SiO_2 and sodium carbonate is common between both the initial

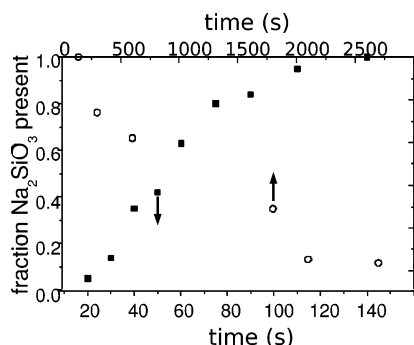


Figure 11. Fraction of crystalline metasilicate, Na_2SiO_3 , present in the isothermal disilicate batch vs time at 850 °C (D850). The buildup (full squares) and decay (open circles) of the intermediate product take place on two different time scales.

$\text{Na}_2\text{O}\text{-SiO}_2$ and $\text{Na}_2\text{O}\text{-}2\text{SiO}_2$ samples. The rate of reaction increases with temperature, but the initial reaction product is independent of temperature in the temperature range studied. The reaction rate is very slow for series M700 with only the formation of Na_2SiO_3 being observed. Only after 41 h of heating, first indications appear of a change of some ^{23}Na product environments away from undistorted metasilicate type. It is apparent from Figure 9 that the rate of reaction is deceleratory, indicating that the reaction is diffusion limited. The reaction product is formed at the point of contact between the SiO_2 and the Na_2CO_3 grains; if the reaction is to continue, the mobile sodium ions must be transported across the increasing layer of product. The amount of Na^+ diffusing from the Na_2CO_3 and depolymerizing the SiO_2 will be decreasing as the Na_2SiO_3 layer increases in thickness. The transport of Na^+ toward the SiO_2 will become too slow for the production of Na_2SiO_3 to continue. Of course, oxygen ions or vacancies also have to diffuse to form Na_2SiO_3 . However, the Na^+ source is restricted to the immediate interface, i.e., the direct grain contact areas, while oxygen can access any part of the open grain surface, where a dynamic equilibrium between oxygen ions, vacancies, and molecular oxygen can be established. The required diffusion length for ionic oxygen species will therefore be small compared to that of Na^+ . It has been reported¹¹ that, as a consequence of this Na^+ diffusion limit, silica-richer phases can be formed at low temperature. Due to the Na^+ concentration gradient caused by the diffusion through the increasing interface layer, there will not be a sudden change in the reaction product from Na_2SiO_3 to $\text{Na}_2\text{Si}_2\text{O}_5$ as we have shown recently by in situ ^{23}Na NMR.¹³ The resonance near -10 ppm in the ^{23}Na spectrum illustrated in Figure 5 for the sample heated for 41 h has a chemical shift that is comparable to published values for crystalline disilicate, $\text{Na}_2\text{Si}_2\text{O}_5$,²⁴ although the line shape observed here differs from that of the stoichiometric crystalline phase obtained by devitrification from the melt. In the present work, the phase is unlikely to be stoichiometric $\text{Na}_2\text{Si}_2\text{O}_5$ due to the Na^+ concentration gradient across the $\text{SiO}_2\text{-Na}_2\text{SiO}_3$ interface layer. Therefore, there will be slightly different ^{23}Na local environments, which will have a slightly different chemical shift. Hence, the line shape will be an average across all the ^{23}Na sites, producing a less well resolved spectrum. However, an occurrence of a new amorphous phase after 41 h would also be consistent with the extra peak found in this spectrum and cannot be ruled out.

The reaction in the $\text{Na}_2\text{O}\text{-}2\text{SiO}_2$ batch series heated at 775 °C (D775) also produces Na_2SiO_3 as a reaction product. The reaction comes to completion in about 60 min by solid-state reaction with no evidence of the formation of any melt phase. The linear relationship between the Na_2CO_3 fraction reacted and

time in Figure 10 indicates that the transport of Na^+ ions across the product layer is not decreasing at this temperature. The rate of reaction increases further for the D850 samples. The reaction proceeds in the same manner as with D775 except that complete reaction of Na_2CO_3 is obtained after 140 s of heating. After the Na_2CO_3 has completely reacted, the production of a silicate melt is observed in the D850 series of experiments. This is evident from both the ^{23}Na and ^{29}Si spectra with the growth of a broad resonance line. The average Q^n species in a $\text{Na}_2\text{O}\text{-}2\text{SiO}_2$ glass should be Q^3 , i.e., $n = 3$;¹⁶ however, this does not imply that only Q^3 species are expected in the glass. In the D850 sample heated for 35 min, about 95 mol % of the sample is glassy and there exist Q^2 , Q^3 , and Q^4 , having a weighted average of $n = 3$. The reaction of Na_2CO_3 in the D850 samples turns deceleratory toward the end of the reaction (Figure 11). This slowing in the rate of reaction of Na_2CO_3 indicates a change in the reaction mechanism toward diffusion control as soon as the reaction between SiO_2 and the crystalline Na_2SiO_3 begins.

5. Conclusions

Quantitative information concerning the formation and evolution of intermediate reaction products has been obtained through a multinuclear combination of NMR techniques. Furthermore, MAS NMR, although being essentially a bulk technique, has been used to gain quantitative information involving a spatially restricted interface layer.

Crystalline Na_2SiO_3 is an early reaction product in both the nonisothermal and isothermal experiments. In the nonisothermal series, evidence of the formation of a $\text{Na}_2\text{O}\text{-}2\text{SiO}_2$ melt at 850 °C is obtained from the broad resonance peak near -90 ppm in the ^{29}Si spectra. At temperatures of 1090 °C and above, the melting of crystalline Na_2SiO_3 is deduced from the broadening of the ^{29}Si spectra. Na_2SiO_3 is also the preferred initial reaction product for the isothermally heated samples M700, D775, and D850. It can be concluded that, once the Na_2SiO_3 layer grows to a critical thickness and the temperature is sufficiently low, the diffusion of Na^+ is decreased to such an extent that not enough Na^+ will reach the SiO_2 to produce more Na_2SiO_3 . This is the case with the M700 series. Silica-richer phases are now being formed in the interface layer between the SiO_2 and $\text{Na}_2\text{-SiO}_3$, with a pronounced Na^+ concentration gradient across the layer. The reaction process of the disilicate and metasilicate samples appears to be a two-step mechanism. The first step for sodium disilicate batch samples is the solid-state reaction between SiO_2 and Na_2CO_3 forming crystalline Na_2SiO_3 . This stage continues until all Na_2CO_3 has reacted. The second stage is the reaction between the SiO_2 and the Na_2SiO_3 forming the $\text{Na}_2\text{O}\text{-}2\text{SiO}_2$ melt. The second stage of the reaction is considerably slower than the first stage. The first stage is complete after 140 s for D850, while the second stage is near completion after 45 min. Therefore, the first melt only appears after all the $\text{Na}_2\text{-CO}_3$ has reacted. A similar two-stage mechanism can be used to describe the reaction of the metasilicate batch. The first stage is again the reaction of SiO_2 and Na_2CO_3 producing Na_2SiO_3 . This continues until no more Na_2SiO_3 can be produced due to a critical thickness of Na_2SiO_3 already formed, preventing sufficient Na^+ ions from reaching the SiO_2 . The second stage sees the production of $\text{Na}_2\text{O}\text{-}2\text{SiO}_2$ at the SiO_2 grain interface layer. Also there will be a significant Na^+ concentration gradient between pure $\text{Na}_2\text{O}\text{-SiO}_2$ and pure $\text{Na}_2\text{O}\text{-}2\text{SiO}_2$ layers. In both cases the reaction product and rate of formation are controlled by the diffusion of Na^+ .

The ^{13}C MAS NMR experiments have revealed a carbonate species that exists at the Na_2CO_3 grain boundary, i.e., at the

reaction interface between SiO₂ and Na₂CO₃. The observed additional peak at 172.1 ppm for the 850 °C sample relates to a carbon species located in the interface layer between the Na₂CO₃ and SiO₂ grains. This species is similar to the Na-carbonate complex that was observed in studies of CO₂ dissolution in melts at high pressure. This species is a transient reaction state on the Na₂CO₃ grain boundary during atomic rearrangements as the reaction proceeds before release of the CO₂ in molecular form. This interpretation is supported by the shorter T_1 value of this carbonate species due to its being in closer proximity to a Fe³⁺ paramagnetic center, and by the change in its chemical shift.

Appendix

To piece together the individual contributions of the components in the nonisothermal batch at 850 °C, we have taken the ratio of the intensities of the metasilicate and carbonate lines from the ²³Na spectrum (Figure 2a)

$$\frac{x_{\text{Na}_2\text{SiO}_3}}{x_{\text{Na}_2\text{CO}_3}} = \frac{39}{78} \quad (1)$$

As the line originating from the distorted Na⁺ environment in carbonate (the broad line to the right) is masked by the glassy contribution (cf. Figure 2b), we have used the integrated intensity of the metasilicate peak for $x_{\text{Na}_2\text{SiO}_3}$ and then rescaled the pure carbonate spectrum to match the sharp carbonate line, so that the integrated intensity of the rescaled spectrum is an accurate measure of $x_{\text{Na}_2\text{CO}_3}$. The contribution from the glassy phase (cf. Figure 2b) is best estimated from the corresponding ²⁹Si spectrum in Figure 1b. Therefore, we have taken the ratio of the intensities of the Q³ glass and metasilicate components from the ²⁹Si spectrum

$$\frac{x_{\text{Q}^3}}{x_{\text{Na}_2\text{SiO}_3}} = \frac{22}{13} \quad (2)$$

The quartz line in the ²⁹Si spectrum is not quantitative and is therefore disregarded here. In addition, we have the molar balance (the molar fractions have to add up to 1)

$$x_{\text{SiO}_2} + x_{\text{Q}^3} + x_{\text{Na}_2\text{SiO}_3} + x_{\text{Na}_2\text{CO}_3} = 1 \quad (3)$$

and the requirement that the average number of bridging oxygens per silicon atom is conserved at $\bar{n} = 2$

$$x_{\text{SiO}_2} + \frac{x_{\text{Q}^3}}{2} = x_{\text{Na}_2\text{CO}_3} \quad (4)$$

Solving the resulting system of equations

$$\begin{pmatrix} 0 & 0 & 78 & -39 \\ 0 & 13 & -22 & 0 \\ 1 & 1 & 1 & 1 \\ 1 & 1/2 & 0 & -1 \end{pmatrix} \begin{pmatrix} x_{\text{SiO}_2} \\ x_{\text{Q}^3} \\ x_{\text{Na}_2\text{SiO}_3} \\ x_{\text{Na}_2\text{CO}_3} \end{pmatrix} = \begin{pmatrix} 0 \\ 0 \\ 1 \\ 0 \end{pmatrix} \quad (5)$$

results in $x_{\text{SiO}_2} = 20\%$, $x_{\text{Q}^3} = 29\%$, $x_{\text{Na}_2\text{SiO}_3} = 17\%$, and $x_{\text{Na}_2\text{CO}_3} = 34\%$.

Acknowledgment. A.R.J. and R.W. thank Dominique Massiot (Centre de Recherche sur les Matériaux à Haute Température, Orléans) for discussion and for the use of the Dmfit software. A.R.J. would like to thank the UK Engineering and Physical Sciences Research Council and Pilkington plc for a Ph.D. studentship from the Collaborative Awards in Science and Engineering scheme.

References and Notes

- (1) Hong, K. S.; Speyer, R. F. *J. Am. Ceram. Soc.* **1993**, 76, 598.
- (2) Suwannathada, P.; Hessenkemper, H. *Glastech. Ber. Glass Sci. Technol. (Offenbach, Ger.)* **1997**, 70, 306.
- (3) Willburn, F. W.; Thomasson, C. V. *J. Soc. Glass. Technol.* **1958**, 42, 158.
- (4) Kautz, K. *Glastech. Ber. Glass Sci. Technol. (Offenbach, Ger.)* **1969**, 42, 244.
- (5) Savard, M. E.; Speyer, R. F. *J. Am. Ceram. Soc.* **1993**, 76, 671.
- (6) Hong, K. S.; Lee, S. W.; Speyer, R. F. *J. Am. Ceram. Soc.* **1993**, 76, 605.
- (7) Dickinson, C. F. Ph.D. Thesis, University of Salford: Manchester, UK, 2000.
- (8) Cable, M.; Martlew, D. *Glastech. Ber. Glass Sci. Technol. (Offenbach, Ger.)* **1988**, 61, 31.
- (9) Savard, M. E.; Speyer, R. F. *Glass Technol.* **1993**, 34, 210.
- (10) Dolan, M. D.; Misture, S. T. *Glass Technol.* **2004**, 45, 167.
- (11) Stoch, L.; Kraishan, S. *Glastech. Ber. Glass Sci. Technol. (Offenbach, Ger.)* **1997**, 70, 298.
- (12) Jones, A. R.; Winter, R.; Greaves, G. N.; Targett-Adams, C.; Smith, I. H. *Glass Technol.* **2002**, 43C, 52.
- (13) Jones, A. R.; Winter, R.; Florian, P.; Massiot, D. *J. Phys. Chem. B* **2005**, 109, 4324.
- (14) Schneider, E.; Stebbins, J. F.; Pines, A. *J. Non-Cryst. Solids* **1987**, 89, 371.
- (15) Dupree, R.; Holland, D.; Mortuza, M. G. *J. Non-Cryst. Solids* **1990**, 116, 148.
- (16) Meneau, F.; Greaves, G. N.; Winter, R.; Vaills, Y. *J. Non-Cryst. Solids* **2001**, 293, 693.
- (17) Jones, A. R.; Winter, R.; Greaves, G. N.; Smith, I. H. *J. Non-Cryst. Solids* **2001**, 293, 87.
- (18) Drake, K. O.; Carta, D.; Skipper, L. J.; Sowrey, F. E.; Newport, R. J.; Smith, M. E. *Solid State Nucl. Magn. Reson.* **2005**, 27, 28.
- (19) Kohn, S. C.; Brooker, R. A.; Dupree, R. *Geochim. Cosmochim. Acta* **1991**, 55, 3879.
- (20) Brooker, R. A.; Kohn, S. C.; Holloway, J. R.; McMillan, P. F.; Carroll, M. R. *Geochim. Cosmochim. Acta* **1999**, 63, 3549.
- (21) Blank, J. G.; Brooker, R. A. *Rev. Miner.* **1994**, 30, 157.
- (22) Morizet, Y.; Brooker, R. A.; Kohn, S. C. *Geochim. Cosmochim. Acta* **2002**, 66, 1809.
- (23) Behrens, H.; Ohlhorst, S.; Holtz, F.; Champenois, M. *Geochim. Cosmochim. Acta* **2004**, 68, 4687.
- (24) Xue, X.; Stebbins, J. F. *Phys. Chem. Miner.* **1993**, 20, 297.
- (25) Massiot, D.; Fayon, F.; Capron, M.; King, I.; LeCalvé, S.; Alonso, B.; Durand, J. O.; Bujoli, B.; Gan, Z.; Hoatson, G. *Magn. Reson. Chem.* **2002**, 40, 70.
- (26) Koller, H.; Engelhardt, G.; Kentgens, A. P. M.; Sauer, J. *J. Phys. Chem.* **1994**, 98, 1544.
- (27) Clark, T. M.; Grandinetti, P. J.; Florian, P.; Stebbins, J. F. *J. Phys. Chem.* **2001**, 105, 12257.
- (28) Mysen, B. O.; Virgo, D. *Am. Miner.* **1980**, 65, 1166.
- (29) Tossell, J. A. *Geochim. Cosmochim. Acta* **1995**, 59, 1299.
- (30) Fine, G.; Stolper, E. *Contrib. Mineral. Petrol.* **1985**, 91, 105.